

required supply voltage of 1.37 V. Below this value the transconductance of the circuit decreases for certain common input voltages. Fig. 5 shows the effective tail currents I_{S_n} and I_{S_p} as well as the sum of these tail currents as a function of the common input voltage V_i . The maximum variation of the sum current is less than 0.25%. The resulting combined transconductance is also shown in Fig. 5 (dashed line) and has a maximum deviation from its nominal value of 5%. This relatively large deviation is due to the different slope factors (eqn. 1) of nMOS and pMOS transistors. Furthermore, the slope factor is also dependent on the source-bulk biasing voltage of the transistors.

Conclusion: An input circuit is presented which gives a common voltage independent transconductance without many extra components (four MOS transistors) and operating without extra supply voltage. The transconductance is constant within 5%.

© IEE 1993

16th April 1993

J. H. Botma, R. F. Wassenaar and R. J. Wiegink (MESA Research Institute, University of Twente, PO Box 217, 7500 AE Enschede, The Netherlands)

References

- HUIJSING, J. H., and LINEBARGER, D.: 'Low-voltage operational amplifier with rail-to-rail input and output ranges', *IEEE J. Solid-State Circuits*, 1985, SC-20, pp. 1144-1150
- FISHER, J. A., and KOCH, R.: 'A highly linear CMOS buffer amplifier', *IEEE J. Solid-State Circuits*, 1987, SC-22, (3), pp. 330-334
- HOGERVORST, R., WIEGERINK, R. J., DE JONG, P. A. L., FONDERIE, J., WASSENAAR, R. F., and HUIJSING, J. H.: 'Low-voltage CMOS opamp with rail-to-rail input and output voltage range'. Proc. ISCAS, 1992, pp. 2876-2879
- PARDOEN, M. D., and DEGRAUWE, M. G.: 'A rail-to-rail input/output CMOS power amplifier', *IEEE J. Solid-State Circuits*, 1990, SC-25, pp. 501-504
- DUQUE-CARRILLO, J. F., PÉREZ-ALOE, R., and MORILLO, A.: 'Push-pull current circuit for biasing CMOS amplifier with rail-to-rail common-mode range', *Electron. Lett.*, 1991, 27, (23), pp. 2122-2125
- VITTOZ, E., and FELLRATH, J.: 'CMOS analog integrated circuits based on weak inversion operation', *IEEE J. Solid-State Circuits*, 1977, SC-12, pp. 224-231

SPATIAL ACTIVE OPTICAL SWITCHING BY USING GRATING COUPLED SURFACE EMITTING DFB LASERS

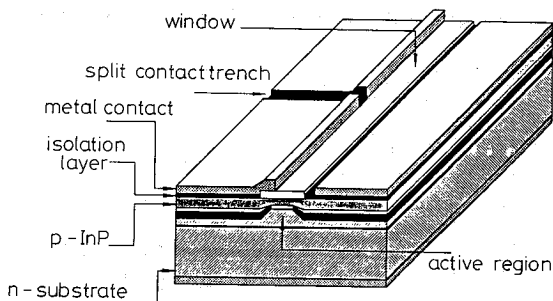
S. F. Yu, R. G. S. Plumb and J. E. Carroll

Indexing terms: Optical switching, Lasers, Optical modulation

Distinct far field patterns have been demonstrated from grating coupled surface emitting distributed feedback lasers which may therefore be employed as two state spatial optical switches with high speed switching potential.

The far field profiles of grating coupled surface emitting DFB lasers depend on the phase and intensity of the longitudinal fields [1], which in turn are functions of the lasing wavelength with respect to the grating period. In passive (DBR type) surface emitters, calculation of grating emission angle is a simple function of wavelength and grating period [2, 3]. To obtain the far-field patterns of DFB lasers we must perform a more complex analysis allowing for carrier induced refractive index changes along the grating, and the more complicated field profiles (we may also include the effects of any deliberate phase jumps). Our previous paper showed theoretically and experimentally that injection of external light could cause far field switching, a wavelength switch being part of the mechanism [4]. The present Letter reports theoretical and experimental demonstration of far field switching by non-uniform current injection via split contacts.

A 1.55 μm InGaAsP BH laser with a second order grating was used for the experiment. Light was allowed out of the laser surface by ion beam etching a window through the contact metal alongside the lasing filament as shown in Fig. 1.



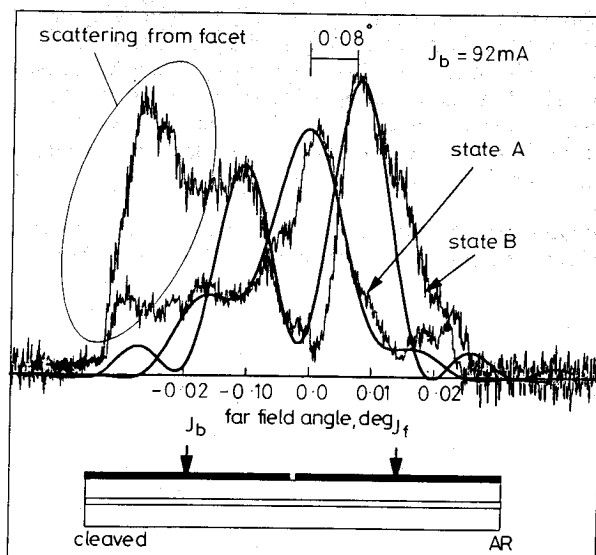
54971

Fig. 1 Schematic diagram of split contacts grating coupled surface emitting DFB laser

About half of the p-contact to the laser was removed by this window, but sufficient remained for lasing to continue without significant departure from the original laser characteristics. The laser was 325 μm long, with the front facet antireflection coated, and the back as-cleaved. Lengths of front, gap, and back sections were 175, 25, and 125 μm , respectively.

The far field of the emission from the top surface of the laser was monitored using the faceplate of an infra-red TV camera. Because the surface emission is very divergent in the direction perpendicular to the stripe, an appropriately focused cylindrical lens was used to improve collection efficiency without significant effect on the far field of interest: i.e. that parallel to the stripe. The faceplate was positioned 65 cm from the laser. Simultaneously with the far-field measurements, light from the antireflection coated facet was coupled via a standard graded index fibre to an optical spectrum analyser.

Fig. 2 illustrates the far-field switching between two bias states. In state A the front drive was 28 mA and the back 92 mA, and an almost single lobed pattern is seen. In state B the back current remained at 92 mA, whereas the front was increased to 42 mA. The latter state is basically double lobed with an angular separation between the lobes of 0.18°, the single lobe from state A falling almost in the centre. The ratio of output in state A to output in state B is over 10:1, measured at the angle for peak output in state A. There is also a spurious lobe seen to the left for state B, which is associated with the longitudinal propagating wave reflected and scattered from the as-cleaved facet; this is difficult to avoid with a window in the p-side of the laser, but has not been observed in any lasers with n-side windows. Shown on the same diagram



54972

Fig. 2 Measured far-field profiles under different current injection profiles

Thick lines: calculated far field profiles

are far fields calculated using a modified power matrix method; agreement with the measured curves is seen to be good, except in the region on the left where the light scattered from the facet occurs as mentioned above.

Fig. 3 shows spectral measurement on the same laser. The dominant wavelength peak has been tracked while the current

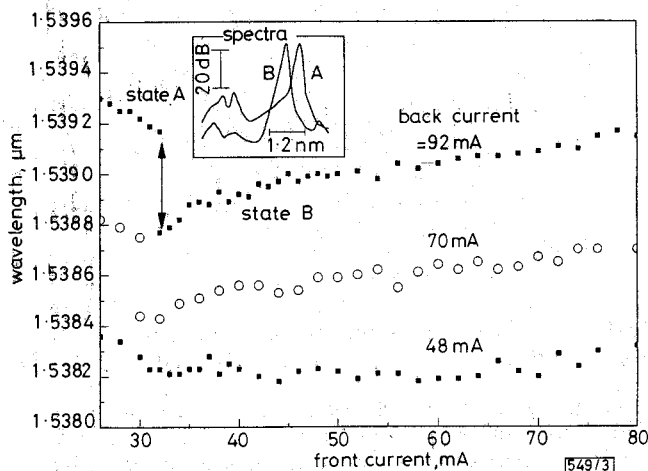


Fig. 3 Lasing wavelength against current injection between the two contacts

in the front section of the laser was varied, keeping the back section current constant. An abrupt change of wavelength is seen at a front current of 32 mA and back current 92 mA, corresponding to the difference between far field states A and B. In this particular device, no hysteresis was observed at the wavelength switching point. Wavelength and far field switching were also observed at the wavelength switching point. Wavelength and far field switching were also observed at a back current of 70 A, but not at 48 mA.

Strictly, far field angles have to be calculated from the full modal state of the resonance laser cavity; however, to a first approximation we may assume that the laser is nonresonant and then calculate the shift in peak far field angles between states A and B from the wavelength shift using

$$\Delta\theta = \sin^{-1}(n_{eff} \Delta\lambda/\lambda_0) \quad (1)$$

where n_{eff} is the effective index of the laser waveguide, $\Delta\lambda$ is the 0.6 nm shift seen in Fig. 3, and λ_0 is the mean wavelength from the same Figure, taken as 1.54 μm . This gives $\Delta\theta = 0.076^\circ$ which is close to the measured value of 0.08° .

In conclusion, we have demonstrated far field spatial switching using electrical control in a surface emitting DFB laser. Predictions from theoretical modelling have shown good agreement with the experimental behaviour. The far-field shape should be improved if the emitting window is opened on the substrate side of the chip (optimisation of facet reflectivity would also help this). Switching high powers should be possible. The fast nature of wavelength switching in DFB lasers [5] suggests that lasers of the type reported (with improvements) could have applications in spatial switching and dynamic optical interconnection.

Acknowledgment: The authors wish to thank M. Robertson from BTL for supplying the laser diode. S. Yu also wishes to

thank the Croucher Foundation of Hong Kong and ORS Award for support.

© IEE 1993

29th March 1993

S. F. Yu, R. G. S. Plumb and J. E. Carroll (Engineering Department, Cambridge University, Trumpington Street, Cambridge CB2 1PZ, United Kingdom)

References

- 1 HENRY, C. H., KAZARINOV, R. F., LOGAN, R. A., and YEN, R.: 'Observation of destructive interference in radiation loss of second-order distributed feedback lasers', *IEEE J. Quantum Electron.*, 1985, **QE-21**, (2), pp. 151-154
- 2 NAGATA, H., KOMABA, N., and YAMASHITA, K.: 'AlGaAs grating surface emitting beam deflector with ridge structure', *IEEE Photonics Technol. Lett.*, 1991, **3**, pp. 222-224
- 3 KOJIMA, K., and KYUMA, K.: 'Fast beam switching in surface-emitting distributed bragg reflector laser', *Appl. Phys. Lett.*, 1988, **53**, (15), pp. 1357-1359
- 4 YU, S. F., ZHANG, L. M., PLUMB, R. G. S., and CARROLL, J. E.: 'Effect of external reflectors on radiation profile of grating coupled surface emitting lasers', *IEE Proc. J*, 1993, **140**, (1), pp. 30-38
- 5 KUZNETSOV, M.: 'Picosecond switching dynamics of a bistable-wavelength-latch two segment distributed feedback laser', *IEEE Photonics Technol. Lett.*, 1990, **2**, pp. 623-625

ERRATA

MITCHELL, H. B., and DORFAN, M.: 'Block truncation coding using Hopfield neural network', *Electron. Lett.*, 1992, **28**, (23), pp. 2144-2145

Authors' corrections

In eqn. 7, the numerator of the last term should read

$$\{\sum x[i](1 - V[i])^2\}$$

KWAN, H. K.: 'New form of delayed N-path recursive digital filters', *Electron. Lett.*, 1993, **29**, (9), pp. 736-738

Printers' corrections

The *Indexing terms* were omitted and should read

Digital filters, Filters, Systolic arrays

Immediately before eqn. 3, insert

Adaptive algorithm: For $M = 2$, taking the inverse z-transform of eqns. 1 and 2, we obtain